Boletim Técnico da Escola Politécnica da USP
Departamento de Engenharia de Telecomunicações
e Controle

ISSN 1517-3550
BT/PTC/0101

Model-Based Soft-Sensor Design for On-Line Estimation of the Biological Activity in Activated Sludge Wastewater Treatment Plants

Oscar A. Z. Sotomayor
Song Wong Park
Claudio Garcia

São Paulo – 2001

FICHA CATALOGRÁFICA

Sotomayor, Oscar Alberto Zanabria
Model-based soft-sensor design for on-line estimation of the biological activity in activated sludge wastewater treatment plants / O.A.Z. Sotomayor, S.W. Park, C. Garcia. – São Paulo : EPUSP, 2001.
37 p. – (Boletim Técnico da Escola Politécnica da USP, Departamento de Engenharia de Telecomunicações e Controle, BT/PTC/0101)

1. Soft-sensor 2. Lodo ativado 3. Esgotos – Estações de tratamento I. Park, Song Wong II. Garcia, Claudio III. Universidade de São Paulo. Escola Politécnica. Departamento de Engenharia de Telecomunicações e Controle IV. Título V. Série
ISSN 1517-3550

CDD 621.381536
628.354
628.162

MODEL-BASED SOFT-SENSOR DESIGN FOR ON-LINE ESTIMATION OF THE BIOLOGICAL ACTIVITY IN ACTIVATED SLUDGE WASTEWATER TREATMENT PLANTS

Oscar A. Z. Sotomayor[1,¥], Song Won Park[1] and Claudio Garcia[2]

Escola Politécnica da Universidade de São Paulo
(1) Department of Chemical Engineering – Laboratory of Simulation and Process Control (LSCP)
(2) Department of Telecommunications and Control Engineering – Laboratory of Automation and Control (LAC)
Av. Prof. Luciano Gualberto, trav. 3, n. 380, Cidade Universitária
CEP 05508-900, São Paulo-SP, Brazil
Phone: +55 11 3818.2237, Fax: +55 11 3813.2380, E-mail: oscar@lscp.pqi.ep.usp.br

Abstract: This paper considers the design of a "soft sensor" (software sensor) for the on-line estimation of the biological activities of a colony of aerobic microorganisms acting on activated sludge processes, where the carbonaceous waste degradation and nitrification processes are taken into account. These bioactivities are intimately related to the Dissolved Oxygen (DO) concentration. Two factors that affect the dynamics of the dissolved oxygen are the respiration rate or the Oxygen Uptake Rate (OUR) and the oxygen transfer function ($K_l a$). These items are challenging topics for the application of recursive identification due the nonlinear characteristic of the oxygen transfer function and to the time-varying feature of the respiration rate. In this work, OUR and the oxygen transfer function are estimated through a "soft sensor", which is based on a modified version of the discrete extended Kalman filter (EKF). Numerical simulations have been carried out in a pre-denitrifying activated sludge process benchmark and the obtained results demonstrate the applicability and efficiency of the proposed methodology, which should provide a valuable tool to supervise and control activated sludge processes.

Keywords: Biosensing, Soft sensors, Bioactivities, Activated sludge process, Dissolved oxygen dynamics, Recursive identification, Extended Kalman filter, Nonlinear systems, Wastewater treatment plants.

¥ Author to whom all correspondence should be addressed.

1. Introduction

The lack of reliable sensors and the high cost of advanced instrumentation are significant problems in the monitoring and control of wastewater treatment plants (WWTP). Despite the intensive research in recent years to develop new sensors for biological applications, the state of available sensors nowadays is not much different than a decade ago. In order to overcome these inconveniences, estimation techniques issued from control and systems theory have been applied in the development of "soft sensors" for on-line estimation of bioprocess variables. A "soft sensor" can be described as the association between a sensor (hardware) and an estimator (software). The estimator is the part that infers the on-line estimation of the variable from measurements made by the sensor.

Wastewater processing by means of activated sludge (AS) is the most widespread sewage biological treatment process and its efficiency depends, besides other factors, on the capacity of a sensitive community of microorganisms. Thus, the availability of on-line information about the microbiological activity is of crucial importance for the monitoring and control of the process. Bioactivities in the activated sludge process are intimately related to the dissolved oxygen (DO) concentration. The heterotrophic bacteria degrade the carbonaceous organic matter employing oxygen to oxidize and mineralize organic matter to produce carbon dioxide. Nitrification (ammonium removal) is made by a special group of autotrophic bacteria, called nitrifiers. In this process, the Nitrosomonas oxidize ammonium into nitrite (nitritification) and the Nitrobacters oxidize nitrite into nitrate (nitratification). In comparison with heterotrophic microorganisms, nitrifiers need more oxygen for their growth, so the nitrification process is often responsible for approximately 40 percent of the total oxygen demand [1]. The dynamics of the nitrification process is slower than the one relative to the process performed by the heterotrophic bacteria. In addition to the heterotrophic and nitrifying bacteria there are other aerobic microorganisms species that also influence the oxygen consumption rate. The autotrophic sulphur bacteria are able to oxidize hydrogen sulphide (or other reduced sulphur compounds) to sulphuric acid. Autotrophic iron bacteria oxidize inorganic ferrous iron to the ferric form to obtain energy [2].

Two factors that affect the dynamics of the dissolved oxygen concentration are the bacterial respiration rate or oxygen uptake rate (OUR) and the oxygen transfer function ($K_l a$). OUR is a meaningful biological indicator [3], that measures the rate at which the microorganisms utilize oxygen in carrying out their metabolic activities. It is directly linked to two important biochemical processes that must be controlled in a wastewater treatment plant: biomass growth and substrate consumption. OUR also provides information about influent waste concentration and composition, and concentration of biodegradable matter in the effluent. Further, a rapid decrease in the respiration rate implies that some forms of toxic elements may have entered the plant, so knowledge of the respiration rate can be used to detect the existence of such toxins and prevent microorganisms from dying. The oxygen transfer function describes the rate at which oxygen is transferred to the wastewater by the aeration equipment, so knowledge of the oxygen transfer function determines the air blowing flow. The oxygen uptake rate may vary significantly in a matter of minutes, whereas oxygen transfer function variations, depending on the state of the aeration equipment and sludge inventory, can occur over a daily time scale [4].

In this paper, OUR and the oxygen transfer function are on-line estimated using a "soft sensor", from measurements of the DO concentration and the air injection flow rate, in a continuous-flow activated sludge process. The model-based "soft sensor" is designed using a modified version of the discrete extended Kalman filter for the simultaneous estimation of the OUR and the oxygen transfer function, assuming that the OUR can be described by a filtered random walk process, while the oxygen transfer function can be modeled by an exponential function. Other papers have used these models to estimate OUR and the $K_l a$ function. Nevertheless, they have only been tested in a simulator with a single equation that describes the dissolved oxygen concentration dynamics, as in [5] or in off-line estimations with data from small pilot plants, as in [6] or [7]. In this paper the "soft sensor" is tested by simulation in the ASWWTP-USP benchmark [8], a dynamic model that simulates all the biological, physical and biochemical interactions that occur in a complete activated sludge plant. In this way the results here obtained are more useful for applications in real systems.

2. Soft sensors

A "soft sensor" is the association of a sensor (hardware), that measures on-line some process variable, with a state estimation algorithm (software) that infers on-line some *hidden* meaningful information from the data provided by the sensor. A critical element in the synthesis of a "soft sensor" is the available knowledge of the process. An accurate process model generally expresses this knowledge. However, it is normally impossible to obtain an exact process model, so that the estimation algorithm must be robust enough to deal with model errors. As regards modeling errors, it is assumed that [9]: (1) the uncertainty arises from imprecision in a set of model parameters, as determined from the physical knowledge of the process; (2) the erroneous model of the process consists of the nominal model with a first-order Taylor series expansion about the nominal parameters; and (3) the parameter errors are white noises with zero mean, normal distribution with a constant covariance matrix that can be determined, and possibly updated, from on-line data. A schematic diagram of a "soft sensor" is shown in Fig. 1.

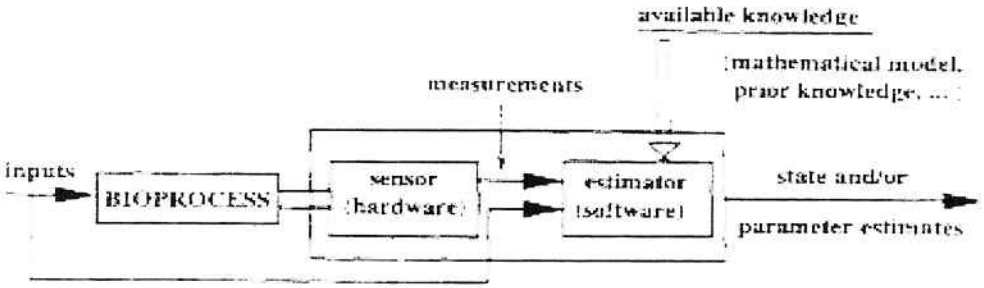

Fig. 1 – Principle of a "soft sensor" [10].

2.1 The software: extended Kalman filter

Several estimation techniques have been proposed in the literature. Among these techniques, three of them have been recognized to have strong potential in the on-line estimation of bioprocesses, namely, (1) estimation through elemental balances; (2) adaptive non-linear observers; and (3) artificial neural networks (ANN). An overview of each technique as well as the most significant applications are presented in [11].

There are four main approaches to the design of nonlinear observers [12]: (1) the extended Kalman filter (EKF); (2) the geometric observer (GO) design; (3) the high-gain (HG) approach; and (4) the sliding-mode (SM) approach. These estimation techniques are restricted to nonlinear plants that are completely open-loop observable, and their extensions to partially observable (i.e. detectable) plants do not seem straightforward, as it can be seen in [13]. A non-exhaustive evaluation of these nonlinear observers and other methods of approach are summarized in Wang et al. [14].

The EKF is by far the most widely used state estimation technique, while the application of the GO, HG, SM and other approaches is a recent and less widespread development [15]. The EKF is simply an ad hoc state estimator that only approximates the optimality of Bayes' rule by linearization. This means that the EKF computes a state estimate at each sampling time by the use of Kalman filter [16,17] on a linearized model of the nonlinear system. This technique is applicable if there is a sufficiently large neighborhood in which the linearized model is a good representation of the nonlinear system. If, in addition, the disturbances are well represented by zero mean Gaussian measurement noise, the optimal estimate of the linearized system should be a reasonable approximation of the optimal estimate for the nonlinear system

Although the EKF is conceptually simple, it has, in practice, three well-known drawbacks [18]:

✓ Linearization can produce highly unstable filter performance (no convergence, biased or divergent estimates) if the timestep intervals are not sufficiently small.

✓ The derivation of the Jacobian matrices is nontrivial in most applications and often lead to significant implementation difficulties.

✓ Sufficiently small timestep intervals usually imply high computational overhead, as the number of calculations demanded for the generation of the Jacobian and the predictions of state estimate and covariance are large.

Despite these problems, the EKF has been successfully used in the development of "soft sensors" in a number of chemical engineering applications, mainly in biotechnology and polymerization. A critical review of experimental applications of EKF in the chemical process industry can be found in Wilson et al. [19].

A number of variants concerning the EKF formulation is possible by modifying the model or the approximation of the probability density function, such as [20]: (1) the first order EKF; (2) the linearized EKF or constant gain EKF; (3) the iterative EKF; (4) the second order EKF; and finally (5) the statistical linearization or quasilinearization method. These options may be presented in the continuous, discrete or continuous-discrete forms. Useful discussions about EKF are available in [21] and [22].

The basic first order EKF is given by the following equation set [23]:

$$e(t) = y(t) - \hat{y}(t) \tag{1}$$

$$K(t) = \frac{FP(t-1)\varphi(t)}{r_2 + \varphi^T(t)P(t-1)\varphi(t)} \tag{2}$$

$$P(t) = \left[F - K(t)\varphi^T(t)\right]P(t-1)F^T + R_1 \tag{3}$$

$$\hat{\theta}(t) = F\hat{\theta}(t-1) + K(t)e(t) \tag{4}$$

where $e(t)$ is the prediction error, $y(t)$ is the output system, $\hat{y}(t)$ is the estimated output system, $K(t)$ is the Kalman gain matrix, $P(t)$ is the prediction error covariance matrix, $\hat{\theta}(t)$ is the estimated parameter/state vector, F is the process state matrix gain, $\varphi(t)$ is the regressor vector, R_1 is the observed noise covariance matrix and r_2 is the measurement noise variance.

2.2 A modified EKF

Recursive least-square estimation (RLS) is the most popular technique for estimating constant or slowly changing parameters. To allow the estimator to maintain its sensitivity to process parameter variations, RLS is often used with an exponential weighting factor (or forgetting factor). Sayed and Kailath [24] showed the exact and complete relationship that exists between the field of Kalman filtering and the field of RLS adaptive filtering, which have been highlighted in [25] and [26] for the EKF case. This close relationship motivates us to adapt the exponential weighting factor to the EKF prediction error covariance matrix. Hence, equations (2) and (3) are replaced by the following expressions:

$$K(t) = \frac{FP(t-1)\varphi(t)}{\lambda + \varphi^T(t)P(t-1)\varphi(t)} \tag{5}$$

$$P(t) = \frac{1}{\lambda}\left\{\left[F - K(t)\varphi^T(t)\right]P(t-1)F^T + R_1\right\} \tag{6}$$

where λ is the exponential weighting factor.

3. The activated sludge plant

The ASWWTP-USP benchmark is a dynamic simulator developed for the evaluation of control strategies in biological wastewater treatment plants. The simulator represents an activated sludge process in a configuration with pre-denitrification for the removal of organic matter and nitrogen from domestic effluent. The process configuration, shown in Fig. 3, is formed by a bioreactor, composed of an anoxic zone (for the denitrification process) and two aerobic zones (for the organic matter degradation and the nitrification process), and a secondary settler (for the clarification/thickening process). The compartments of the bioreactor are considered to have constant volume (13 m^3, 18 m^3 and 20 m^3, respectively) and to be ideally mixed whereas the secondary settler (20 m^3) is modeled employing a series of 10 layers (one-dimensional model, where it is assumed that no biological reaction occurs). The influent flow Q_{in} is 4.17 m^3/h, with a proportion of biodegradable matter of 224 mg

COD/l and a hydraulic retention time of 17.0 hours. The internal recycle flow rate $Q_{int} = 2Q_{in}$, the external recycle flow rate $Q_{sl} = 0.5Q_{in}$, the wastage flow rate $Q_w = 0.0258$ m^3/h and the external carbon source flow rate $Q_{ext} = 0$ m^3/h. The airflow rates are: $Q_{air_2} = 0.044$ m^3/h and $Q_{air_3} = 0.033$ m^3/h, for the first and second aerobic zones, respectively. In the anoxic zone, no airflow rate is considered.

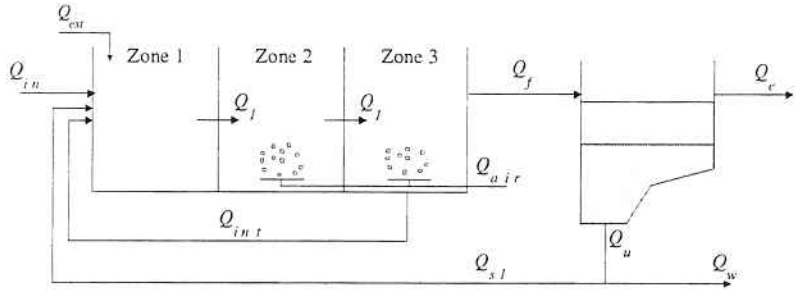

Fig. 2 – Layout of the ASWWTP-USP benchmark [8].

For the objectives of this work, it is important to use a model that realistically simulates a true plant. Here, each bioreactor zone is modeled by IAWQ Activated Sludge Model N°1, abbreviated ASM1, presented by Henze et al. [27] and the secondary settler is modeled by the double exponential settling velocity model presented by Takács et al. [28]. The complete plant model includes approximately 52 coupled, complex and nonlinear differential equations, which were implemented in Simulink/Matlab platform v.5.3 [29]. The values of the process parameters are shown in Table 1 and Table 2, and the wastewater composition (average values) is shown in Table 3. A major explanation concerning the simulator can be found in [8].

In this paper, it is emphasized the dissolved oxygen concentration in the zone 3 of the bioreactor.

Table 1
Parameter values of the ASM1 for a temperature of 15°C [30]

Symbol	Value	Description
Y_H	0.67 g cell COD formed/(g COD oxidized)	Yield for heterotrophic biomass
Y_A	0.24 g cell COD formed/(g N oxidized)	Yield for autotrophic biomass
f_p	0.08 (dimensionless)	Fraction of biomass yielding particulate products
i_{XB}	0.08 g N/(g COD) in biomass	Mass of nitrogen per mass of COD in biomass
i_{XP}	0.06 g N/(g COD) in endogenous mass	Mass of nitrogen per mass of COD in products from biomass in endogenous mass
μ_H	0.1667 h^{-1}	Maximum specific growth rate for heterotrophic biomass
b_H	0.0125 h^{-1}	Decay rate coefficient for heterotrophic biomass
K_S	10 g COD/m^3	Half saturation coefficient for heterotrophic biomass
K_{OH}	0.2 g O_2/m^3	Oxygen half saturation coefficient for heterotrophic biomass
K_{NO}	0.5 g NO_3-N/m^3	Nitrate half saturation coefficient for denitrifying heterotrophic biomass
μ_A	0.02083 h^{-1}	Maximum specific growth rate for autotrophic biomass
b_A	0.002083 h^{-1}	Decay rate coefficient for autotrophic biomass
K_{OA}	0.4 g O_2/m^3	Oxygen half saturation coefficient for autotrophic biomass
K_{NH}	1.0 g NH_3-N/m^3	Ammonium half saturation coeficient for autotrophic biomass
n_g	0.8 (dimensionless)	Correction factor for μ_H under anoxic conditions
k_a	0.0033 m^3/(g COD.h)	Ammonification rate
k_h	0.002083 g biod. COD/(g COD.h)	Maximum specific hydrolysis rate
K_X	0.1 g biod. COD/(g COD)	Half saturation coefficient for hydrolysis of slowly biodegradable substrate
n_h	0.8 (dimensionless)	Correction factor for hydrolysis under anoxic conditions

Table 2
Operational and design parameters for the Takács settler [8]

Symbol	Value	Description
v_0	19.75 m/h	Maximum theoretical settling velocity
v_0'	10.42 m/h	Maximum practical settling velocity
r_h	5.76 x 10^{-4} l/mg	Settling parameter associated with the hindered settling component of settling velocity equation
r_p	2.86 x 10^{-3} l/mg	Settling parameter associated with the low concentration and slowly settling component of the suspension
f_{ns}	2.28 x 10^{-3} (dimensionless)	Non-settleable fraction of the influent suspended solids
X_{min}	$f_{ns} \cdot X_{SS,f}$ mg/l	Min. attainable suspended solids concentration in the effluent
X_t	3000 mg/l	Threshold suspended solids concentration
A	20 m^2	Surface area of clarifier
h	0.1 m	Height of the each layer
n	10 (dimensionless)	Number of layers
m	7 (dimensionless)	Number of the feedlayer
f_1	0.75 (dimensionless)	Conversion factor of solids suspended (SS) to COD
f_2	0.75 (dimensionless)	Conversion factor of SS to COD

Table 3
Inflow wastewater concentration (average values) [8]

Variable	Value	Description
X_{BH}	20.0 *mg COD/l*	Active heterotrophic biomass
X_{BA}	0.0 *mg COD/l*	Active autotrophic biomass
X_S	160.0 *mg COD/l*	Slowly biodegradable substrate
X_{ND}	18.28 *mg N/l*	Particulate biodegradable organic nitrogen
X_{IP}	40.0 *mg COD/l*	Particulate inert matter & products
S_O	0.0 *mg (-COD)/l*	Dissolved oxygen concentration
S_{NH}	12.5 *mg N/l*	Soluble ammonium (and ammonia) nitrogen
S_{ND}	10.1 *mg N/l*	Soluble biodegradable organic nitrogen
S_{NO}	1.0 *mg N/l*	Soluble nitrate (and nitrite) nitrogen
S_S	64.0 *mg N/l*	Readily biodegradable substrate
S_{ALK}	7.0 *m mol/l*	Total alkalinity

4. The dissolved oxygen (DO) dynamics

The dynamics of the dissolved oxygen is such that its concentration can change in a matter of minutes. To illustrate some of the problems in the dynamics of the dissolved oxygen concentration, its differential equation extracted from the IAWQ model is analyzed. The rigorous ASM1 equation that describes the dissolved oxygen concentration is given by the following expression [31]:

$$\frac{dS_O}{dt} = -\mu_H\left(\frac{1-Y_H}{Y_H}\right)\left(\frac{S_S}{K_S+S_S}\right)\left(\frac{S_O}{K_{OH}+S_O}\right)X_{BH} - \\ -\mu_A\left(\frac{4.57-Y_A}{Y_A}\right)\left(\frac{S_{NH}}{K_{NH}+S_{NH}}\right)\left(\frac{S_O}{K_{OA}+S_O}\right)X_{BA} + \\ K_l a\cdot\left(S_{O,sat}-S_O\right)+D_{in}S_{O,in}-D_{out}S_O \tag{7}$$

As can be observed in Eq. (7) the gain of the process depends on the substrate concentrations S_{NH} and S_S, and on the biomass concentration X_{BH} and X_{BA}. It also depends on time-varying parameters such as μ_H, μ_A, Y_H, Y_A, K_{NH}, K_{OA}, K_{OH} and K_S, the saturated oxygen concentration $S_{O,sat}$ (that depends on pressure, temperature, certain characteristics of the wastewater, etc), the input oxygen concentration $S_{O,in}$, the dilution rates (flow/volume) D_{in} and D_{out}, and the oxygen transfer

function $K_l a$. The oxygen transfer function in a real plant depends on several factors, for example, airflow rate, type of diffusers, wastewater composition, temperature, pressure, design of aeration tank, tank depth, spatial distribution and efficiency of aeration devices, etc. Other factors that affect the DO concentration dynamics are: oxygen concentration in the different flows inside the plant, flow and composition of the influent, inclusion of unaerated zones for nutrient removal, recycle of activated sludge and mixed liquor and operating sludge age.

4.1 A suitable continuous model

In an activated sludge process, the biodegradable substrate is consumed by the microorganisms, which utilize oxygen to carry out their bioactivities. Due to the many uncertainties in Eq. (7), here it will be adopted the following reduced order model proposed by Bastin and Dochain [32], that describes the DO concentration of a completely mixed tank:

$$\frac{dS_O}{dt} = -OUR + K_l a \cdot \left(S_{O,sat} - S_O\right) + D_{in} S_{O,in} - D_{out} S_O \tag{8}$$

This model can be regarded as bilinear and includes, besides mass balance and addition of oxygen caused by aeration system, the term *OUR* (oxygen uptake rate or respiration rate), as described by the conceptual model structure shown in Fig. 3.

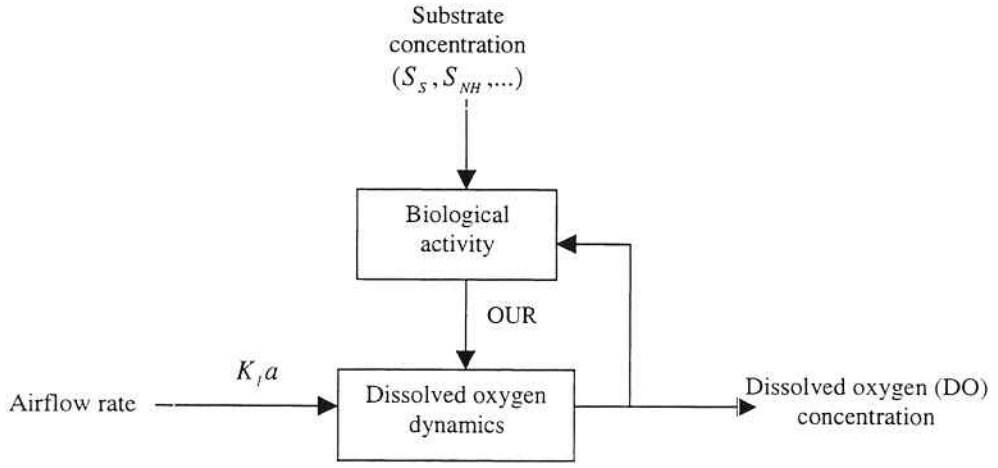

Fig. 3. Conceptual relation between biological activity and DO concentration.

The importance of *OUR* as an indicator of bioactivities was first suggested by Olsson and Andrews [33] and Stenstrom and Andrews [34] and several results became available soon after, regarding the estimation of *OUR* and also $K_l a$. The respiration rate is time varying, normally diurnal (and cannot be assumed to be slowly time varying or constant). Typically, it has a daily variation around a nonzero mean value, but it may change abruptly, in a matter of minutes, due to disturbances. The oxygen transfer function depends on several factors, as mentioned before, but the main time-varying dependence is with the airflow rate [7].

4.2 The discrete model

A discrete-time model corresponding to continuous-time DO model is obtained using a zero-order-hold sampler [35]. This technique assumes that all signals except $S_O(t)$ are constant during the sampling interval, what is reasonable for sufficiently fast sampling.

Zero-order-hold sampling of the DO concentration dynamics has been previously presented in earlier works [5, 7, 36, 37]. The application is completely derived here. Thus, from Eq. (8), assuming constant volume, we have:

$$\frac{dS_O(t)}{dt} = -OUR(t) + K_l a(\cdot)\cdot S_{O,sat}(t) - K_l a(\cdot)\cdot S_O(t) + D(t)\cdot S_{O,in}(t) - D(t)\cdot S_O(t) \tag{9}$$

Now considering that:

$$M(t) = -\left(K_l a(\cdot) + D(t)\right) \tag{10}$$

and

$$N(t) = -OUR(t) + D(t)\cdot S_{O,in}(t) + K_l a(\cdot)\cdot S_{O,sat} \tag{11}$$

then Eq. (9) can be written in the following way:

$$\frac{dS_O(t)}{dt} = N(t) + M(t)\cdot S_O(t) \tag{12}$$

Assuming that $M(t)$ and $N(t)$ are constant within each sampling interval and applying the Laplace transform to Eq. (12):

$$S_O(s) = \frac{N}{s(s-M)} + \frac{S_O(0)}{(s-M)} \tag{13}$$

Given the state in the sampling time "t_k", the state in some future time "t" has the following form:

$$S_O(t) = -\frac{N}{M} + \frac{N}{M}e^{M\cdot(t-t_k)} + S_O(t_k)\cdot e^{M\cdot(t-t_k)} \tag{14}$$

therefore, the state in the next sampling time "t_{k+1}" is:

$$S_O(t_{k+1}) = -\frac{N}{M} + \frac{N}{M} e^{M\cdot(t_{k+1}-t_k)} + S_O(t_k)\cdot e^{M\cdot(t_{k+1}-t_k)} \tag{15}$$

Considering $\Delta t = t_{k+1} - t_k$ the sampling period and simplifying the notation replacing "t_k" by "t", Eq. (15) results:

$$S_O(t+1) = S_O(t)\cdot e^{M(t)\cdot\Delta t} + \frac{N(t)}{M(t)}\left(e^{M(t)\cdot\Delta t} - 1\right) \tag{16}$$

Making:

$$T_s = \frac{1}{M(t)}\left(e^{M(t)\cdot\Delta t} - 1\right) \tag{17}$$

Eq. (16) may be rewritten as:

$$\begin{aligned} S_O(t+1) = S_O(t) + T_s \cdot \big[& -OUR(t) + K_l a(\cdot)\cdot\left(S_{O,sat} - S_O(t)\right) + \\ & D(t)\cdot\left(S_{O,in}(t) - S_O(t)\right)\big] + e_{DO}(t) \end{aligned} \tag{18}$$

where the term $e_{DO}(t)$ has been added to describe measurement noise, sampling and model errors. Here it is possible to prove, employing Taylor series, that if Δt is small then it is possible to consider $T_s \approx \Delta t$. Taking Δt instead of T_s corresponds to a finite difference approximation of the derivative. The advantage of using T_s as time-varying, is that the sampling period can be made larger. This gives a more appropriate model since higher order dynamics can be neglected [38].

In this work the continuous measurements are digitized using a sampling period Δt, and Eq. (18) with time-varying sampling period T_s, defined in Eq. (17), is used in the implementation of the "soft sensor".

5. Estimation of the DO concentration dynamics

The estimation of $K_l a$ and OUR is not easy. Different approaches have been suggested to estimate these parameters. However, if $K_l a$ is known a priori, the OUR value can be determined quite reliably from the DO mass balance presented in Eq. (8). On the other hand, if OUR is accurately known, the $K_l a$ can be obtained from an input/output gas mass balance, since any input airflow variation produces a variation in the DO concentration, that resembles a first-order dynamics [3], as can be clearly seen in Fig. 4. For the second approach, OUR can be measured by a respirometer [39] or it can be also inferred from na on/off DO control approach [40]. In that case, both $K_l a$ and OUR are simultaneously estimated.

5.1 Definition of the mathematical model

In order to complete the model of Eq. (18) to make it useful for the purposes of this paper, it is necessary that the models of $K_l a$ and OUR be defined.

The oxygen transfer function has been approximated in different ways, as discussed in Bennett [41]. Usually the following assumptions are made, regarding the $K_l a$ function [42]:

1. $K_l a$ can be sufficiently well described as a function of the airflow rate.
2. The parameters of $K_l a$ change slowly in comparison with the respiration rate.
3. In most cases it is assumed that $K_l a$ is null for zero airflow rates.

A variety of physical models to represent $K_l a$ with a brief summary of applications in the wastewater treatment process is presented in Table 4.

Table 4
Different models for the oxygen transfer function

Model	Equation	References
Step	$K_l a = [0, k_1]$	[43], [44]
Linear A	$K_l a = k_1 \cdot u$	[38], [45], [46]
Linear B	$K_l a = k_1 \cdot u + k_2$	[47], [48], [49], [50], [51]
Arctan	$K_l a = k_1 \cdot \tan^{-1}(k_2 \cdot u)$	[5], [7]
Square root	$K_l a = k_1 \cdot \sqrt{u}$	(Suggested in [38])
Power	$K_l a = k_1 \cdot u^{k_2}$	[52]
Exponential	$K_l a = k_1 \cdot (1 - \exp(-k_2 \cdot u))$	[5], [6], [7], [53], [54]
Polynomial	$K_l a = k_1 \cdot u + k_2 \cdot \sqrt{u} + k_3$	[53], [55], [56]
Piecewise linear	$K_l a = (k_1 + k_2 \cdot t) \cdot u$	[3], [4], [53], [57], [58]
Cubic spline	$K_l a = f(u)$	[7], [53]

In table 4, u is the airflow rate and k_1, k_2 and k_3 are parameters. Here an exponential $K_l a$ model is used, therefore:

$$K_l a\left(Q_{air_3}(t)\right) = k_1 \cdot \left(1 - \exp(-k_2 \cdot Q_{air_3}(t))\right) \tag{19}$$

Regarding OUR, some papers have considered it as being constant [45]. Other authors have modeled OUR as a time-varying parameter ($OUR(t) = R(t)$) [38], what is a very crude approach that may derive biased estimates. A more robust approach considers that OUR can be represented by a time-series approximation, as in [4] and [46]:

$$OUR(t) = b_0 + b_1 \cdot t$$

where the coefficients $\{b_0, b_1\}$ are constant. Due to the time-varying nature of the respiration rate, a "default" description is to model it as a random walk model, which is reasonable, when no specific information is available, thus [57, 58]:

$$OUR(t) = OUR(t-1) + e_{OUR}(t)$$

where $e_{OUR}(t)$ is white noise with zero mean. Random walk models have been widely used in several areas of economy, statistics, physics, chemistry and biology, including modeling of migration of microorganisms [59]. Some modifications of random walks, as the integrated and filtered random walk models, have been suggested and have occasionally set profoundly difficult mathematical problems.

In general applications, a filtered random walk model gives a better tracking than a random walk model or an integrated random walk model [60]. Since a bad tracking of *OUR* also influences in the $K_l a$ parameters estimation, here it will is used the following filtered random walk model for the respiration rate [5, 6]:

$$OUR(t) = \frac{1}{(1 - pz^{-1})(1 - z^{-1})} e_{OUR}(t) \tag{20}$$

where p is a filter parameter. (z^{-1} represents the backward shift operator, defined as $z^{-1}OUR(t) = OUR(t-1)$).

In the following discussions, the dynamics of the DO sensors and the airflow valve characteristic were neglected. Nevertheless, the DO sensors can be modeled as a first-order system [39, 61], and the actuator dynamic can easily be incorporated in the $K_l a$ model [62].

5.2 Design of the "soft sensor"

Having defined the mathematical model for the dynamics of the dissolved oxygen concentration, it is possible now to design the "soft sensor" for the simultaneous estimation of the respiration rate and of the oxygen transfer function in zone 3 of the bioreactor. Taking into account the exponential model of the oxygen transfer function, defined in Eq. (19), the unknown parameter vector has the form:

$$\theta_{K_l a}(t) = [k_1 \quad k_2]^T \tag{21}$$

Supposing that K_1a is time varying, then it is possible to write this variation by a random walk model, in the following manner:

$$\theta_{K_1a}(t) = F_{K_1a} \cdot \theta_{K_1a}(t-1) + G_{K_1a} \cdot e_{K_1a}(t) \tag{22.1}$$

where $e_{K_1a}(t)$ is zero mean white noise. Eq. (22.1) can be explicitly written as:

$$\begin{bmatrix} k_1(t) \\ k_2(t) \end{bmatrix} = \begin{bmatrix} 1 & 0 \\ 0 & 1 \end{bmatrix} \cdot \begin{bmatrix} k_1(t-1) \\ k_2(t-1) \end{bmatrix} + \begin{bmatrix} 1 \\ 1 \end{bmatrix} \cdot e_{K_1a}(t) \tag{22.2}$$

On the other hand, considering the filtered random walk model of the respiration rate, defined in Eq. (20), OUR can be written as:

$$OUR(t) = (1+p) \cdot OUR(t-1) - p \cdot OUR(t-2) + e_{OUR}(t) \tag{23}$$

Rewriting Eq. (23) in a state space form, which is useful for the Kalman filter, results in:

$$\theta_{OUR}(t) = F_{OUR} \cdot \theta_{OUR}(t-1) + G_{OUR} \cdot e_{OUR}(t) \tag{24.1}$$

or

$$\begin{bmatrix} OUR(t) \\ OUR(t-1) \end{bmatrix} = \begin{bmatrix} 1+p & -p \\ 1 & 0 \end{bmatrix} \cdot \begin{bmatrix} OUR(t-1) \\ OUR(t-2) \end{bmatrix} + \begin{bmatrix} 1 \\ 0 \end{bmatrix} \cdot e_{OUR}(t) \tag{24.2}$$

Now, putting Eqs. (22) and (24) together, it is obtained an expression with the structure of Eq. (4) of the EKF, where the new parameter vector θ and the new process state matrix gain F become implicitly defined in the following equation:

$$\begin{bmatrix} k_1(t) \\ k_2(t) \\ OUR(t) \\ OUR(t-1) \end{bmatrix} = \begin{bmatrix} 1 & 0 & 0 & 0 \\ 0 & 1 & 0 & 0 \\ 0 & 0 & 1+p & -p \\ 0 & 0 & 1 & 0 \end{bmatrix} \cdot \begin{bmatrix} k_1(t-1) \\ k_2(t-1) \\ OUR(t-1) \\ OUR(t-2) \end{bmatrix} + \begin{bmatrix} 1 & 0 \\ 1 & 0 \\ 0 & 1 \\ 0 & 0 \end{bmatrix} \cdot \begin{bmatrix} e_{K_l a}(t) \\ e_{OUR}(t) \end{bmatrix} \tag{25}$$

As the system is non-linear, the regressor is derived from the gradient of the prediction error as:

$$\varphi^T(t,\theta(t-1)) = -\left(\frac{de(t,\theta(t-1))}{d\theta(t-1)}\right) \tag{26}$$

where the prediction error is defined as:

$$e(t) = S_O(t) - \hat{S}_O(t) \tag{27}$$

with $S_O(t)$ being the real value and $\hat{S}_O(t)$ the estimated value of the dissolved oxygen concentration in zone 3 of the bioreactor. Using Eq. (18) for the predicted DO concentration in time "t" and inserting it in Eq. (27) results:

$$\begin{aligned} e(t) = S_O(t) - \Big\{ & S_O(t-1) + T_s \cdot \Big[-\hat{OUR}(t-1) + \hat{K}_l a(Q_{air_3}(t-1)) \cdot (S_{O,sat} - S_O(t-1)) + \\ & D(t-1) \cdot (S_{O,in}(t-1) - S_O(t-1)) \Big] \Big\} \end{aligned} \tag{28}$$

Therefore, the regressor vector is obtained according to:

$$\varphi^T(t,\theta(t-1)) = T_s \cdot \left[\left(S_{O,sat} - S_O(t-1)\right) \cdot \frac{d\hat{K}_l a(Q_{air_3}(t-1))}{d\theta(t-1)} - \frac{d\hat{OUR}(t-1)}{d\theta(t-1)} \right] \tag{29}$$

$$\varphi(t,\theta(t-1)) = T_s \cdot \begin{bmatrix} \left(S_{O,sat} - S_O(t-1)\right) \cdot \left(1 - \exp(-\alpha(t))\right) \\ \left(S_{O,sat} - S_O(t-1)\right) \cdot \beta(t) \cdot \exp(-\alpha(t)) \\ -1 \\ 0 \end{bmatrix} \tag{30}$$

with:

$$\alpha(t) = k_2 \cdot Q_{air_3}(t-1) \tag{31}$$

$$\beta(t) = k_1 \cdot Q_{air_3}(t-1) \tag{32}$$

Eqs. (25), (28), (30), (31) and (32) form the "soft sensor".

5.3 Selection of probing input signals

The importance of the specific probing signal is now considered. It is well know that reliable parameter estimates can be obtained only if the input is persistently exciting, otherwise the lack of an adequately updated input may produce an ill-conditioned covariance matrix ($P(t)$) and consequently an estimator failure [63].

Dissolved oxygen (DO) concentration in aerated tanks is typically controlled by manipulation of the airflow rate, which is implicitly represented in Fig. 3. Fig. 4 shows how the DO concentration, in zone 3 of the bioreactor, reacts to airflow rate changes. The non-linear effect of the airflow rate in the DO concentration is clearly seen.

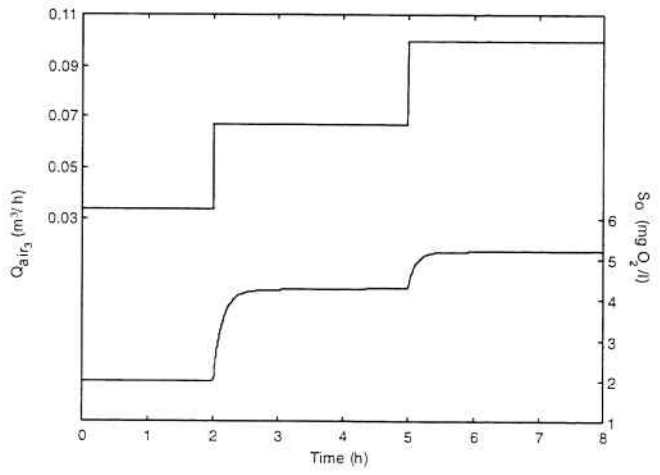

Fig. 4. Upper part: Airflow rate variation. Lower part: DO response

From an engineering point of view, it would be unjustifiable to alter the airflow rate just to guarantee persistent excitation, because this quantity is normally adjusted in order to meet the operation requirements of the process and cannot be varied at will. From a practical point of view, it would be desirable to perform the estimation by simply varying the airflow rate from a minimum to a maximum value at prescribed time intervals, with open or closed loop. In closed loop it is necessary to include an additional signal to the airflow rate or an on/off control.

The limits of variation in the airflow rate are very important and they are related to the oxygen demand of the process. The DO concentration has to be sufficiently high so that the growth of heterotrophic and autotrophic bacteria is not limited due to lack of oxygen. Usually the autotrophic microorganisms are more sensitive to low concentrations than the heterotrophic microorganisms. Excessively high DO concentrations increase energy consumption and deteriorate the process performance since they reduce the sludge quality and make the denitrification (in a nutrient removal process) less efficient, due to the internal recycle. Likewise, low DO concentrations lead to bad quality sludge and less efficient pollutant removal.

Biological degradation of carbonaceous organic matter occurs when the DO concentration is above a threshold limit of about 1 mg O_2/l (equivalent to 1 mg (-COD)/l using the units of the model). On the other hand, nitrification requires higher oxygen concentrations. Nitritification needs oxygen concentrations higher than 3 mg O_2/l, while the nitratification requires more than 5.5 mg O_2/l for optimal results. The right DO concentration is always a balance between economic and biological needs, however practical experience shows that 2 mg O_2/l is usually a good choice for satisfactory performance.

Here, in order to generate rapid changes in the DO concentration to obtain good estimates, without strongly influencing the process performance, the signal input corresponds to open-loop random disturbances in the airflow rate Q_{air_3}, between 0.01 and 0.09 m^3/h which cause variations in the DO concentration in the zone 3 between 0.5 and 5 mg O_2/l. These disturbances have a negligible effect

in the DO concentration in zone 2 of the bioreactor, which is kept almost constant in its nominal value of 2 mg O_2/l. The airflow rate was changed each 8.3 min, corresponding to the time constant of the process in open loop (τ_{open}) for a 100% variation in the nominal value of Q_{air_3} . In a typical large scale plant the nominal dissolved oxygen concentration time constant is about 20-30 minutes [42]. In this paper all the signals were sampled with a sampling period $\Delta t = 0.1 \cdot \tau_{open} = 49.8 \text{sec}$. The DO measurements are considered uniform in the zones (in a real plant it depends on the location of the sensor) and it is assumed that the saturated oxygen concentration is $S_{O,sat} = 8.65$ mg O_2/l.

The large variations in the airflow rate used for the estimation and the corresponding dissolved oxygen concentration are shown in Fig. 5. To test the estimator with more realistic conditions, simulations with noise measurements were performed. A Gaussian process (white noise with zero mean and standard deviation 0.05) was generated and added to the dissolved oxygen concentration produced by the benchmark. A time horizon of 8 hours was considered sufficient for this study based on simulation.

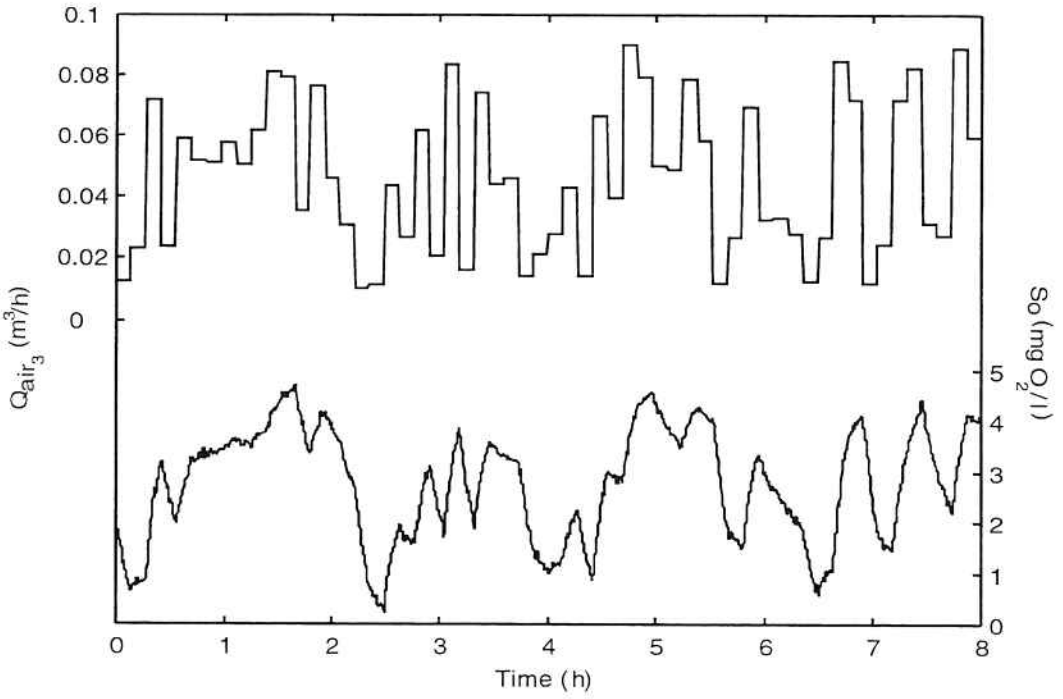

Fig. 5. Data input for estimation. Upper part: Airflow rate variation in zone 3.
Lower part: Dissolved oxygen concentration in zone 3.

5.4 Choice setup conditions

Before starting to test the "soft sensor" it is necessary to determine the initial conditions and the value of some parameters in the estimation algorithm. Some criteria were used to choose these initial conditions and these parameters are next presented.

1. Choosing $\hat{\theta}(0)$ and $P(0)$

The initial estimated vector $\hat{\theta}(0)$ is usually adjusted to zero, unless some *a priori* information is available. The initial covariance matrix $P(0)$ is normally specified as a diagonal matrix $P(0)=cI$, where c is a large positive number, such as 10^4 or 10^6, which indicates the diffidence of the user in choosing $\hat{\theta}(0)$, besides providing a fast convergence of the estimated parameters. Small values of c make $\hat{\theta}(t)$ to change slowly.

2. Choosing R_1

The matrix R_1 represents the covariance matrix of the observed noise $e_\theta(t)$ and reflects the variations of the time-varying parameters in $\theta(t)$ and has, in general, to be tried out. Setting $R_1=0$ implies no tracking capability, since $K(t)$ goes to zero when $t\to\infty$. Hence to be able to track time-varying parameters it is necessary to set $R_1>0$.

From equation (25):

$$e_\theta(t)=G\cdot\begin{bmatrix} e_{K_{Id}}(t) \\ e_{OUR}(t) \end{bmatrix}$$

Then, the covariance matrix R_1 is defined as:

$$R_1 = Ee_\theta(t)e_\theta^T(t) = \begin{bmatrix} Ee_{K_1a}^2(t) & \overline{0} \\ \overline{0} & GG^T Ee_{OUR}^2(t) \end{bmatrix} \tag{33}$$

As $Ee_{K_1a}^2(t)$ and $Ee_{OUR}^2(t)$ are usually unknown, normally R_1 is taken as a constant diagonal matrix of the form:

$$R_1 = \begin{bmatrix} a_1 & 0 & 0 & 0 \\ 0 & a_2 & 0 & 0 \\ 0 & 0 & a_3 & 0 \\ 0 & 0 & 0 & a_4 \end{bmatrix} \tag{34}$$

The diagonal elements of R_1 are determined by trial and error, considering the compromise between sensibility to time variations and rejection to noise effects. These diagonal elements influence, in different forms, the estimates of the parameters of K_1a (assumed as constant or very slowly changing) and the time-varying respiration rate. a_1 and a_2 are related to the rate of change of the parameters of the oxygen transfer function. Assigning large values for these parameters causes a bias in tracking the respiration rate. Here they are set to zero. a_3 reflects the rapid variation of the respiration rate. A large value provides a faster tracking but generates more noise effects. On the other hand a small value provides a slower tracking but derives less noise effects. a_3 also depends on the filter pole in the filtered random walk model. If p is close to 1, a smaller a_3 should be selected. a_4 is always set to zero, due to the model adopted for *OUR*.

3. Choosing p

The filter pole p is used to adjust the phase of the time variation of the respiration rate. It is chosen to be between 0.9 and 1. When p is close to 1, the estimated respiration rate is greatly affected

by noise. As mentioned before, the choice of p is strongly related to the choice of the element a_3 in matrix R_1, both of them related to the estimation of *OUR*.

4. Choosing λ

In the basic EKF algorithm, r_2 represents the variance of the measurement noise $e_{DO}(t)$, and it is defined as:

$$r_2 = Ee_{DO}(t)e_{DO}^T(t) = Ee_{DO}^2(t) \tag{35}$$

Generally $Ee_{DO}^2(t)$ is unknown, which makes difficult its implementation. This inconvenient is resolved by the use of the factor λ in the modified EKF, since the practical considerations of how using λ are better knowns.

As can be seen in Eq. 6, the effect of exponential weighting factor ($0 < \lambda \leq 1$) is to prevent the elements of $P(t)$ from becoming too small. This makes the filter more sensitive to deviations between the actual and estimated outputs, improving the adjustment of $\hat{\theta}(t)$. On the other hand, when the output y and the input u are close to zero (no excitation), then $P(t-1)\varphi(t) \to 0$ and $K(t) \to 0$. Hence $P(t)$ grows exponentially until $\varphi(t)$ changes. When $\lambda = 1$, all data are weighted equally, generating a slower convergence but providing a better robustness against noise effects. When $0 < \lambda < 1$, more weight is placed on recent measurements than on older ones, deriving a rapid convergence but with more noise influence.

Selecting $\lambda = 1$, the robustness against noise is provided through the choice of the parameter a_3 in R_1. If $\lambda < 1$, the matrix R_1 is affected and, therefore, a bad tracking of *OUR* and biased $K_l a$ - parameters are obtained.

All those criteria must be carefully taken into account to obtain an adequate performance, since the value selected for a parameter will influence the choice of the others. After a series of simulations, the following setup conditions were chosen, as shown in Table 5.

Table 5
Setup conditions used in the simulations

Description	Value
Initial parameter vector	$\theta(0) = [10 \quad 10 \quad 10 \quad 10]^T$
Initial covariance matrix factor	$c = 10^6$
Observed noise covariance matrix element	$a_3 = 0.013$
OUR filter pole	$p = 0.93$
Forgetting factor	$\lambda = 1$

5.5 Performance evaluation of simulation results

As mentioned previously, the "soft sensor" was tested in the ASWWTP-USP benchmark, which simulates all the biological and biochemical phenomena that occur in a real activated sludge plant. The estimation procedure is implemented according to the block diagram shown in Fig. 6, which is a good approach because the model is kept in the traditional continuous form while the measurements are conveniently digitized using a zero-order hold network, reflecting what might be the implementation of a real case.

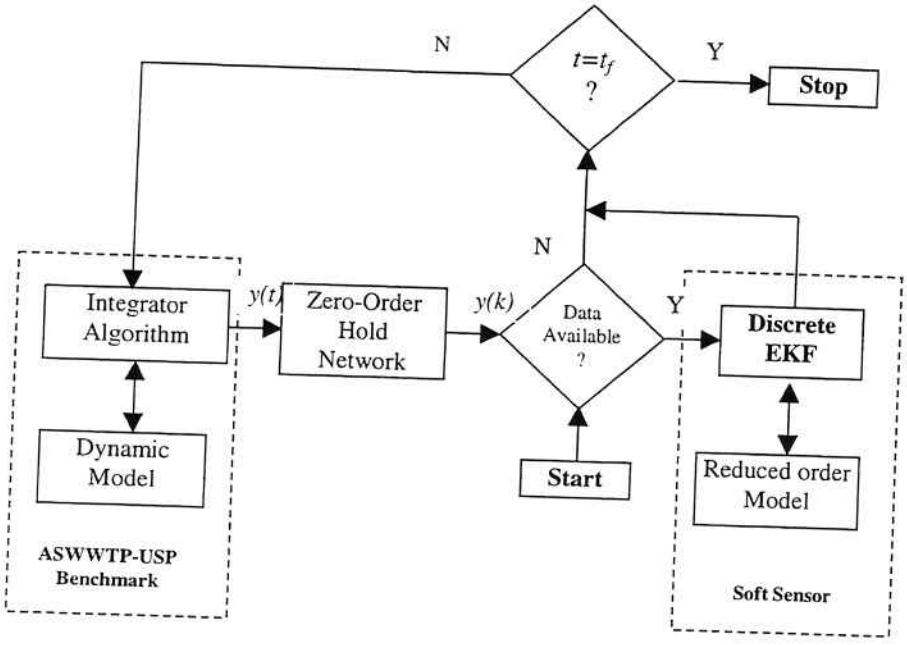

Fig. 6. Software implementation of the estimation procedure.

The performance of the "soft sensor" to estimate the respiration rate and the oxygen transfer function is discussed next. As can be seen in Fig. 7, the estimation of *OUR* and the $K_l a$ -parameters are unbiased. The upper part shows how the estimator, after a short period, tracks very well the changes of the respiration rate. The middle part presents the good fitting of the nonlinear oxygen transfer function. In this case, the estimated oxygen transfer function is obtained with the last estimated value of the $K_l a$ -parameters, i.e. $k_1 = 12.0759$ h^{-1} and $k_2 = 10.0343$ h/m^3, and compared with the $K_l a$ function implemented in the benchmark ($k_1 = 12.5$ h^{-1} and $k_2 = 10.08$ h/m^3). Although using a much higher airflow rate than in the estimation, the curves were quite similar. The lower part shows the excellent fitting between the measured and estimated DO concentration. The time variation of the amplitude of the sampling period T_s is shown in Fig. 8.

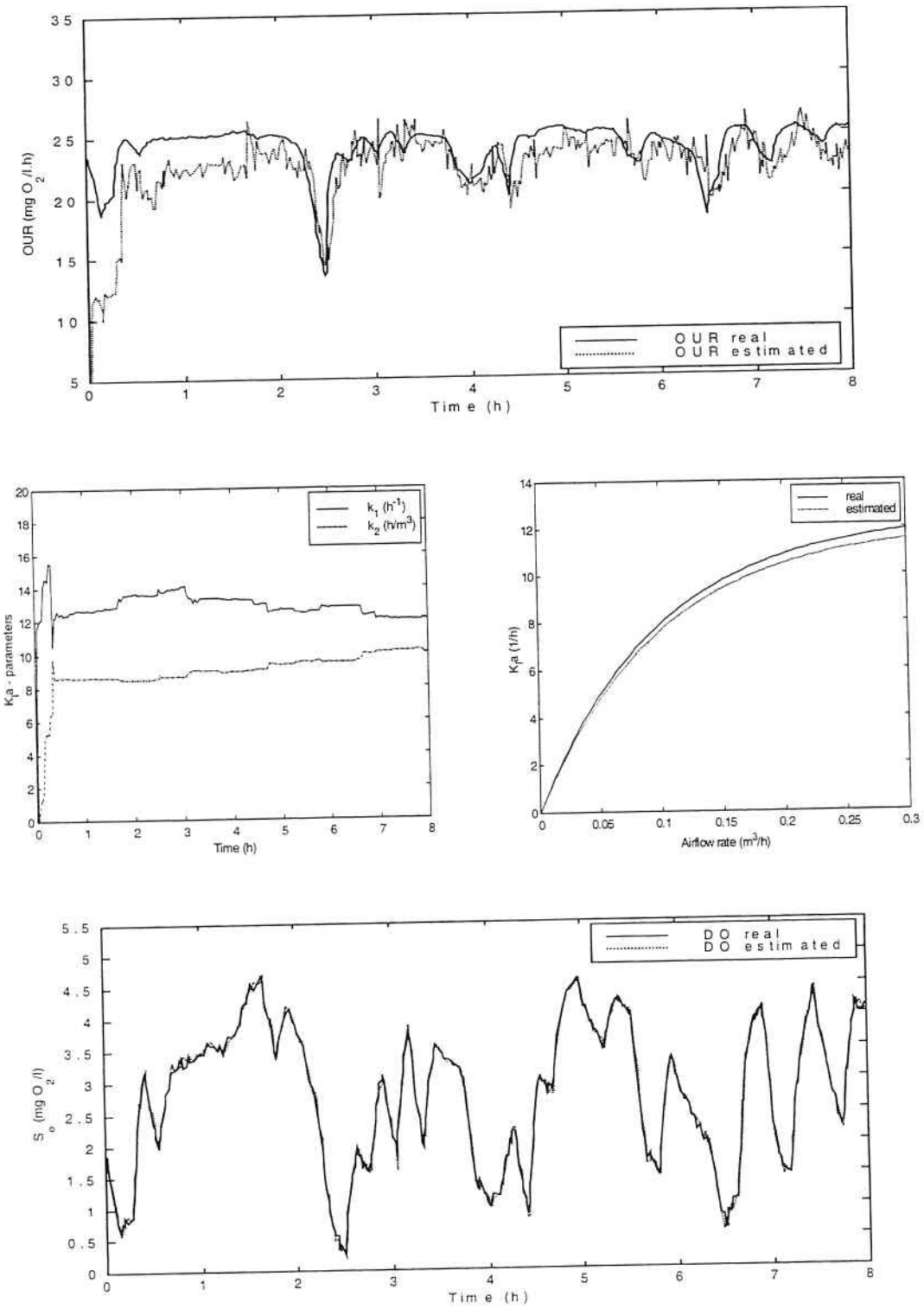

Fig. 7. Responses of the DO estimation. Upper part: Real and estimated respiration rate. Middle part: estimated $K_l a$ -parameters and real and estimated oxygen transfer function. Lower part: Real and estimated DO concentration

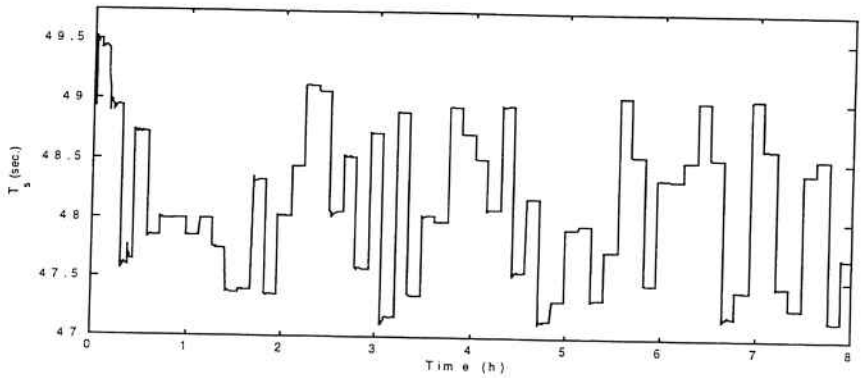

Fig. 8. Time-varying sampling period.

The results obtained with time-varying sampling period are compared with the results obtained using $T_s = \Delta t$, as shown in Table 6, where a discrete version of the integral square error (ISE) is used as performance index (J). The use of $T_s = \Delta t$ generated a biased estimation of *OUR*, what affected mainly the estimation of the parameter k_2. This fact deteriorated the estimation of the system dynamics, increasing the value of the performance indexes.

Table 6
Comparison of performance using a time-varying sampling period (T_s) according Eq. (17) and a constant sampling time $T_s = \Delta t$

$K_l a$ **-parameters and performance index**	**Estimated with time-varying** T_s	**Estimated with** $T_s = \Delta t$
$k_1 = 12.5\ \text{h}^{-1}$	12.0759	12.0730
$k_2 = 10.08\ \text{h/m}^3$	10.0343	9.4592
$J_{K_l a} = \Delta t \cdot \sum_{i=1} (K_l a(i) - \hat{K}_l a(i))^2$	0.5563	1.2947
$J_{OUR} = T_s(i) \cdot \sum_{i=1} (OUR(i) - \hat{OUR}(i))^2$	251.0387	352.6668
$J_{DO} = T_s(i) \cdot \sum_{i=1} (S_O(i) - \hat{S}_O(i))^2$	0.2475	0.2624

Despite a small variation rate in T_s (around 2 seconds), the simulations have shown that the results obtained with a time varying T_s were much better than the ones using a constant T_s.

Applying the estimated values of the parameters k_1 e k_2 in Eq. (19) that describes the oxygen transfer function and using Eq. (18) that describes the mass balance of the DO concentration, it is possible to monitor on-line the oxygen transfer function and the respiration rate. Those two variables may be utilized to implement advanced control strategies, as respirometry based-control.

As an application example, it is shown in Fig. 9 the values of OUR and the $K_l a$ function calculated from the estimated parameters $k_1 = 12.0759$ h^{-1} and $k_2 = 10.0343$ h/m^3, for airflow variations according to Fig. 5. The calculated OUR signal is filtered using a first-order exponential digital filter of the form:

$$OUR_f(t) = \alpha \cdot OUR_c(t) + (1-\alpha) \cdot OUR_f(t-1) \tag{36}$$

with $\alpha = 0.15$.

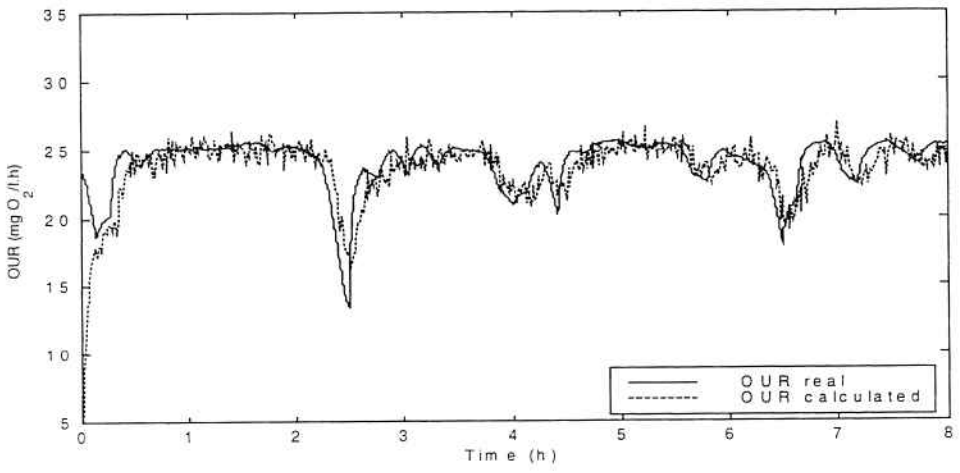

6. Conclusions

In this paper, the biological activity of a colony of aerobic microorganisms present in a pre-denitrifying activated sludge process, is inferentially estimated through a "soft sensor" developed for the simultaneous estimation of the bacterial respiration rate and the oxygen transfer function.

The only need of previous knowledge about the complex dynamics of the dissolved oxygen concentration in the activated sludge process corresponds to a mass balance mathematical model, where the respiration rate is modeled using a filtered random walk model and the oxygen transfer function is modeled by an exponential model. As the estimation algorithm it was employed a modified version of a discrete EKF with time-varying sampling period. The data were acquired from an activated sludge process benchmark, that simulates a real plant. The obtained results have shown that the used methodology was successful in estimating both OUR and the $K_l a$ function.

In a real application the estimation procedure has to be executed in two steps. First, an estimation, as the one developed in this paper, where the simultaneous estimation of OUR and $K_l a$ is performed aiming to obtain a model of the oxygen transfer function. Second, the obtained model of $K_l a$ is used to calculate OUR employing Eq. (8), that describes the mass balance of the dissolved oxygen. In this way it would be possible to get an on-line estimate of the microbial activity in the biological system related to effluent treatment. So, the "soft sensor" here presented constitutes a valuable tool to monitor and control the activated sludge process.

Acknowledgements – The authors acknowledge the financial support by a fellowship from Fundação de Amparo à Pesquisa do Estado de São Paulo (FAPESP), Brazil, under process n. 98/12375-7: Control and On-line Optimization Applied to Activated Sludge Treatment Systems.

References

[1] H. Spanjers, P.A. Vanrolleghem, G. Olsson, P. Dold, Respirometry in control of the activated sludge process, Water Science and Technology 34 (3-4) (1996) 117-126.

[2] H. Spanjers, P.A. Vanrolleghem, G. Olsson, P. Dold, Respirometry in control of the activated sludge process: principles. Scientific and Technical Report No. 7, IAWQ, London, 1998.

[3] S. Marsili-Libelli, A. Vaggi, Estimation of respirometric activities in bioprocesses, Journal of Biotechnology 52 (3) (1997) 181-192.

[4] S. Marsili-Libelli, Adaptive estimation of bioactivities in the activated sludge process, IEE Proc. Control Theory and Applications 137 (6) (1990) 349-356.

[5] S. Nakajima, C.-F. Lindberg, B. Carlsson, On-line estimation of the respiration rate and the oxygen transfer function using an extended Kalman filter. Technical Report IR-S3-REG-9613, Royal Institute of Technology, Sweden, 1996.

[6] C.-F. Lindberg, B. Carlsson, Estimation of the respiration rate and oxygen transfer function utilizing a slow DO sensor, Water Science and Technology 33 (1) (1996) 325-333.

[7] C.-F. Lindberg, Control and estimation strategies applied to the activated sludge process. PhD. Thesis, Uppsala Unversity, Sweden, 1997.

[8] O.A.Z. Sotomayor, S.W. Park, C. Garcia, A general benchmark for simulation of innovating control strategies in biological wastewater treatment plants, Brazilian Journal of Chemical Engineering (2000), (Submitted).

[9] G. Leu, R. Baratti, An extended Kalman filtering approach with a criterion to set its tuning parameters; application to a catalytic reactor, Computers and Chemical Engineering 24 (2-7) (2000) 1839-1849.

[10] A.J. de Assis, R.M. Filho, Soft sensors development for on-line bioreactor state estimation, Computers and Chemical Engineering 24 (2-7) (2000) 1099-1103.

[11] M. Farza, H. Hammouri, S. Othman, K. Busawon, Nonlinear observers for parameter estimation in bioprocesses, Chemical Engineering Science 52 (23) (1997) 4251-4267.

[12] J. Alvarez, Nonlinear state estimation with robust convergence, Journal of Process Control 10 (1) (2000) 59-71.

[13] J. Tsinias, Futher results on the observer design problem, Systems & Control Letters 14 (5) (1990) 411-418.

[14] G.-B. Wang, S.-S. Peng, H.-P. Huang, A sliding observer for nonlinear process control, Chemical Engineering Science 52 (5) (1997) 787-805.

[15] J. Alvarez, T. López, Robust dynamic state estimation of nonlinear plants, AIChE Journal 45 (1) (1999) 107-123.

[16] R.E. Kalman, A new approach to linear filtering and prediction problems, Trans. ASME J. Basic Engng., Ser. D, 82 (1960) 35-45.

[17] R.E. Kalman, R.S. Bucy, New results in linear filtering and prediction theory, Trans. ASME J. Basic Engng., Ser. D., 83 (1961) 95-107.

[18] S.J. Julier, J.K. Uhlmann, H.F. Durrant-Whyte, A new approach for filtering nonlinear systems, American Control Conference, Seattle, Washington (1995) 1628-1632.

[19] D.I. Wilson, M. Agarwal, D.W.T. Rippin, Experiences implementing the extended Kalman filter on an industrial bath reactor, Computer & Chemical Engineering 22 (11) (1998) 1653-1672.

[20] F.J. Doyle, Nonlinear inferential control for process applications, Journal of Process Control 8 (5-6) (1998) 339-353.

[21] A.H. Jazwinski, Stochastic Processes and Filtering Theory. Academic Press, New York, 1970.

[22] A. Gelb, J.F. Kasper Jr., R.A.Nash Jr., C.F. Price, A.A. Sutherland Jr., Applied Optimal Estimation. MIT Press, Cambridge, Mass., 1974.

[23] L. Ljung, T. Söderström, Theory and Practice of Recursive Identification. MIT Press, Cambridge, Mass., 1983.

[24] A.H. Sayed, T. Kailath, A state-space approach to adaptive RLS filtering, IEEE Signal Processing Magazine 11 (3) (1994) 18-60.

[25] G.C. Goodwin, K.S. Sin, Adaptive Filtering Prediction and Control. Prentice-Hall, Englewood Cliffs, NJ, 1984.

[26] L. Ljung, System Identification – Theory for the User. 2nd. Ed., Prentice Hall PTR, Upper Saddle River, NJ, 1999.

[27] M. Henze, C.P.L. Grady, W. Gujer, G.v.r. Marais, T. Matsuo, Activated sludge model No. 1. Scientific and Technical Report No. 1, IAWPRC, London, 1987.

[28] I. Takács, G.G. Patry, D. Nolasco, A dynamic model of clarification-thickening process, Water Research 25 (10) (1991) 1263-1271.

[29] Matlab v.5.3 and Simulink v.3.0 – A Program for Simulating Dynamic Systems, The MathWorks Inc., Natick, USA, 1999.

[30] Cost Action 624, Optimal management of wastewater systems. The European Co-operation in the Field of Scientific and Technical Research. Website (http://www.ensic.u-nancy.fr/COSTWWTP/).

[31] U. Jeppsson, Modelling aspects of wastewater treatment processes. PhD. Thesis, Lund Institute of Technology, Sweden, 1996.

[32] G. Bastin, D. Dochain, On-line Estimation and Adaptive Control of Bioreactors. Elsevier, Amsterdam, 1990.

[33] G. Olsson, J.F. Andrews, Dissolved-oxygen profile – valuable tool for control of activated-sludge process, Water Research 12 (11) (1978) 985-1004.

[34] M.K. Stenstrom, J.F. Andrews, Real-time control of activated-sludge process, Journal of the Environmental Engineering Division – ASCE 105 (2) (1979) 245-260.

[35] K.J. Åström, B. Wittenmark, Computer-Controller Systems – Theory and Design. 3rd. Ed., Prentice Hall, Upper Saddle River, NJ, 1997.

[36] S.C. Cook, P.W. Jowitt, Investigation of dissolved oxygen dynamics in the activated sludge process, IFAC Identification and System Parameter Estimation, York, UK, 1985.

[37] U. Holmberg, On the identifiability of dissolved oxygen concentration dynamics, IAWPRC's 25th Anniversary Conference and Exhibition, Kyoto, Japan, 1990.

[38] U. Holmberg, G. Olsson, B. Andersson, Simultaneous DO control and respiration estimation, Water Science and Technology 21 (10-11) (1989) 1185-1195.

[39] H. Spanjers, Respirometry in activated sludge. PhD. Thesis, Wageningen Agricultural University, The Netherlands, 1993.

[40] J. Suescun, I. Irizar, X. Ostolaza, E. Ayesa, Dissolved oxygen control and simultaneous estimation of oxygen uptake rate in activated-sludge plants, Water Environment Research 70 (3) (1998) 316-322.

[41] G.F. Bennett, Oxygen-transfer rates, mechanisms and applications in biological wastewater-treatment, CRC Critical Reviews in Environmental Control 9 (4) (1980) 301-392.

[42] G. Olsson, B. Newell, Wastewater Treatment Processes: Modelling, Diagnosis and Control. IWA Publishing, London, 1999.

[43] S.Y.C. Catunda, G.S. Deep, A.C. van Haandel, R.C.S. Freire, Método de medição contínua da taxa de respiração em sistemas de lodo ativado, XI Brazilian Automatic Control Conference, São Paulo, 1 (1996) 269-273.

[44] S.Y.C. Catunda, G.S. Deep, A.C. van Haandel, R.C.S. Freire, Métodos Alternativos para medição da taxa de consumo de oxigênio em sistemas de lodo ativado, SBA Controle & Automação 9 (2) (1998) 57-64.

[45] K.Y.-J. Ko, B.C. McInnis, G.C. Goodwin, Adaptive control and identification of the dissolved oxygen process, Automatica 18 (6) (1982) 727-730.

[46] S. Marsili-Libelli, Modelling, identification and control of the activated sludge process, Advances in Biochemical Engineering and Biotechnology, 38 (1989) 89-148.

[47] A. Holmberg, Microprocessor-based estimation of oxygen utilization in the activated-sludge wastewater-treatment process, Int. Journal of Systems Science 12 (6) (1981) 703-718.

[48] A. Holmberg, Modeling of the activated-sludge process for microprocessor-based state estimation and control, Water Research 16 (7) (1982) 1233-1246.

[49] A. Holmberg, J. Ranta, Procedures for parameter and state estimation of microbial growth process models, Automatica 18 (2) (1982) 181-193.

[50] G.J. Haarsma, Robust predictive oxygen control – The development of a robust model predictive dissolved oxygen controller for an activated sludge process. MSc Thesis, Wageningen Agricultural University, The Netherlands, 1995.

[51] G.J. Haarsma, K. Keesman, Robust model predictive dissolved oxygen control, 9th Forum for Applied Biotechnology, Belgium, (1995) 2415-2425.

[52] C.Y. Chen, J.A. Roth, W.W. Eckenfelder, Response of dissolved-oxygen to changes in influent organic loading to activated-sludge systems, Water Research 14 (10) (1980) 1449-1457.

[53] C.-F. Lindberg, B. Carlsson, Evaluation of some methods for identifying the oxygen transfer rate and the respiration rate in an activated sludge process. Technical Report UPTEC 93032R, Uppsala University, Sweden, 1993.

[54] G. Olsson, U. Jeppsson, C. Rosén, Control of biological wastewater treatment, Lecture notes, Lund Institute of Technology, Sweden, 1999. Available from http://www.iea.lth.se/sbr/sbre.html.

[55] L.J.S. Lukasse, K.J. Keesman, G. van Straten, Grey-box identification of dissolved oxygen dynamics in activated sludge processes, 13th IFAC World Congress, USA, N (1996) 485-490.

[56] L.J.S. Lukasse, Control and identification in activated sludge processes. PhD. Thesis, Wageningen Agricultural University, The Netherlands, 1999.

[57] B. Carlsson, T. Wigren, On-line identification of the dissolved oxygen dynamics in an activated sludge process, 12th IFAC World Congress, Australia, 7 (1993) 421-426.

[58] B. Carlsson, C.-F. Lindberg, S. Hasselblad, S. Xu, On-line estimation of the respiration rate and the oxygen transfer rate at Kungsängen wastewater treatment plant in Uppsala, Water Science and Technology 30 (4) (1994) 255-263.

[59] G.H. Weiss, Random walks and their applications, American Scientist 71 (1983) 65-71.

[60] L. Ljung, S. Gunnarsson, Adaptation and tracking in system identification – a survey, Automatica 26 (1) (1990) 7-21.

[61] H. Spanjers, G. Olsson, Modeling of the dissolved-oxygen probe response in the improvement of the performance of a continuous respiration meter, Water Research 26 (7) (1992) 945-954.

[62] C.-F. Lindberg, B. Carlsson, Nonlinear and set-point control of the dissolved oxygen concentration in an activated sludge process, Water Science and Technology 34 (3-4) (1996) 135-142.

[63] T. Söderström, P. Stoica, System Identification. Prentice-Hall International, Hemel Hempstead, UK, 1989.

BOLETINS TÉCNICOS - TEXTOS PUBLICADOS

BT/PTC/9901 – Avaliação de Ergoespirômetros Segundo a Norma NBR IEC 601-1- MARIA RUTH C. R. LEITE, JOSÉ CARLOS TEIXEIRA DE B. MORAES

BT/PTC/9902 – Sistemas de Criptofonia de Voz com Mapas Caóticos e Redes Neurais Artificiais – MIGUEL ANTONIO FERNANDES SOLER, EUVALDO FERREIRA CABRAL JR.

BT/PTC/9903 – Regulação Sincronizada de Distúrbios Senodais – VAIDYA INÉS CARRILLO SEGURA, PAULO SÉRGIO PEREIRA DA SILVA

BT/PTC/9904 – Desenvolvimento e Implementação de Algoritmo Computacional para Garantir um Determinado Nível de Letalidade Acumulada para Microorganismos Presentes em Alimentos Industrializados – RUBENS GEDRAITE, CLÁUDIO GARCIA

BT/PTC/9905 - Modelo Operacional de Gestão de Qualidade em Laboratórios de Ensaio e Calibração de Equipamentos Eletromédicos – MANUEL ANTONIO TAPIA LÓPEZ, JOSÉ CARLOS TEIXEIRA DE BARROS MORAES

BT/PTC/9906 – Extração de Componentes Principais de Sinais Cerebrais Usando Karhunen – Loève Neural Network – EDUARDO AKIRA KINTO, EUVALDO F. CABRAL JR.

BT/PTC/9907 – Observador Pseudo-Derivativo de Kalman Numa Coluna de Destilação Binária – JOSÉ HERNANDEZ LÓPEZ, JOSÉ JAIME DA CRUZ, CLAUDIO GARCIA

BT/PTC/9908 – Reconhecimento Automático do Locutor com Coeficientes Mel-Cepstrais e Redes Neurais Artificiais – ANDRÉ BORDIN MAGNI, EUVALDO F. CABRAL JÚNIOR

BT/PTC/9909 – Análise de Estabilidade e Síntese de Sistemas Híbridos – DIEGO COLÓN, FELIPE MIGUEL PAIT

BT/PTC/0001 – Alguns Aspectos de Visão Multiescalas e Multiresolução – JOÃO E. KOGLER JR., MARCIO RILLO

BT/PTC/0002 – Placa de Sinalização E1: Sinalização de Linha R2 Digital Sinalização entre Registradores MFC- PHILLIP MARK SEYMOUR BURT, FERNANDA CARDOSO DA SILVA

BT/PTC/0003 – Estudo da Técnica de Comunicação FO-CDMA em Redes de Fibra Óptica de Alta Velocidade – TULIPA PERSO, JOSÉ ROBERTO DE A. AMAZONAS

BT/PTC/0004 – Avaliação de Modelos Matemáticos para Motoneurônios – DANIEL GUSTAVO GOROSO, ANDRÉ FÁBIO KOHN

BT/PTC/0005 – Extração e Avaliação de Atributos do Eletrocardiograma para Classificação de Batimentos Cardíacos – ELDER VIEIRA COSTA, JOSÉ CARLOS T. DE BARROS MORAES

BT/PTC/0006 – Uma Técnica de Imposição de Zeros para Auxílio em Projeto de Sistemas de Controle – PAULO SÉRGIO PIERRI, ROBERTO MOURA SALES

BT/PTC/0007 – A Connected Multireticulated Diagram Viewer – PAULO EDUARDO PILON, EUVALDO F. CABRAL JÚNIOR

BT/PTC/0008 – Some Geometric Properties of the Dynamic Extension Algorithm – PAULO SÉRGIO PEREIRA DA SILVA

BT/PTC/0009 – Comparison of Alternatives for Capacity Increase in Multiple-Rate Dual-Class DS/CDMA Systems – CYRO SACARANO HESI, PAUL ETIENNE JESZENSKY

BT/PTC/0010 – Reconhecimento Automático de Ações Faciais usando FACS e Redes Neurais Artificiais – ALEXANDRE TORNICE, EUVALDO F. CABRAL JÚNIOR

BT/PTC/0011 – Estudo de Caso: Tornando um Projeto Testável Utilizando Ferramentas Synopsys – REINALDO SILVEIRA, JOSÉ ROBERTO A. AMAZONAS

BT/PTC/0012 – Modelos Probabilísticos para Rastreamento em Carteiras de Investimento – HUGO G. V. DE ASSUNÇÃO, OSWALDO L. V. COSTA

BT/PTC/0013 – Influência de um Controle Imperfeito de Potência e Monitoramento da Atividade Vocal na Capacidade de Sistemas DS/CDMA – MÁRCIO WAGNER DUARTE ROLIM, PAUL JEAN ETIENNE JESZENSKY

BT/PTC/0014 – Canceladores de Interferência Sucessivo e Paralelo para DS/CDMA – TAUFIK ABRÃO, PAUL JEAN E. JESZENSKY

BT/PTC/0015 – Transmissão de Serviços de Multimídia num Sistema Móvel Celular CDMA de Banda Larga – EDUARDO MEIRELLES MASSAUD, PAUL JEAN ETIENNE JESZENSKY

BT/PTC/0016 – Disseminação do HIV em uma População Homossexual Heterogênea – MARCOS CASADO CASTÑO, JOSÉ ROBERTO CASTILHO PIQUEIRA

BT/PTC/0017 – Implementação e Avaliação em Laboratório de um Monitor Cardíaco Portátil para Três Derivações – RAISA FERNÁNDEZ NUNEZ, JOSE CARLOS TEIXEIRA DE BAROS MORAES

BT/PTC/0018 – Projeto de Filtros Recursivos de N-ésima Banda – IRINEU ANTUNES JÚNIOR, MAX GERKEN

BT/PTC/0019 – Relative Flatness and Flatness of Implicit Systems – PAULO SÉRGIO PEREIRA DA SILVA, CARLOS CORRÊA FILHO

BT/PTC/0020 – Estimativa de Fluxo Sangüíneo nas Artérias Coronárias Usando Imagens de Cineangiocardiografia – ANA CRISTINA DOS SANTOS, SÉRGIO SHIGUEMI FURUIE

BT/PTC/0021 – Modelos Populacionais para AIDS e Análise do Equilíbrio sem Epidemia – ELIZABETH FERREIRA SANTOS, JOSÉ ROBERTO CASTILHO PIQUEIRA